XLI CILAMCE
XLI Ibero-Latin American Congress on Computational Methods in Engineering
16-19 November, 2020 FOZ DO IGUAÇU PARANÁ - BRAZIL

Boundary Mesh-Free Model for potential problems

Amanda Araújo[1], Fernando Martins[1], Artur Portela[1]

[1]*PECC – Pós-Graduação em Estruturas e Construção Civil, Department of Civil and Environmental Engineering. University of Brasília, CEP 70910-900, Brasília-DF, Brazil.*
amanda.as96@gmail.com, fernandofilho337@gmail.com, a3portela@gmail.com

Abstract. Within the engineering field, many problems are described by the Laplace Equation, which does not have an analytical solution for complex geometries and boundary conditions. Therefore, numerical methods are highly important for obtaining approximate solutions for problems of this nature. The most utilized numerical methods nowadays involve a mesh for the discretization step, which lead to a high computational cost. This work proposes a Boundary Mesh-Free Model (BMFM) that combines the Boundary Integral Equations and the shape functions generated by the Moving Least Square (MLS) method. This way, the presented method minimizes the need of discretization and eliminates the need of a mesh. The proposed formulation was then applied to a benchmark potential problem governed by the Laplace equation. The results obtained using the BMFM had a small error when compared to the analytical ones, showing how promising the method is.

Keywords: Boundary Mesh-Free Model, Mesh-free Method, Laplace Equation.

1 Introduction

Within the engineering field, many stationary situations can be described by the Laplace equation, such as fluid flows and temperature distribution fields. This differential equation, however, does not have an analytical solution for complex problems. In this context, the numerical methods are highly useful, since they lead to approximate solutions with small errors. At the present day, the most used numerical method is the Finite Element Method (FEM). Nonetheless, FEM still presents some limitations, such as: the possibility of occurrence of exaggerated element distortions, and the loss of accuracy in the recovery of secondary variables. Furthermore, there is a high computational cost associated with the generation of the mesh, see Andújar et al. [1].

The Boundary Element Method (BEM) is an interesting alternative to FEM, since it diminishes the need of discretization. Other advantages of BEM are: easy modelling of infinite domains; higher accuracy than FEM in problems that involve flux concentrations and also in the recovery of secondary variables. However, BEM presents disadvantages, such as: it requires the knowledge of a fundamental solution of the differential equation; it generates non-symmetric and non-sparse matrices; if nodes are not well positioned, elements can still become distorted; and it is not well-suited for solving non-linear problems, as seen in Gaul et al. [2]. Also, even though significantly lower than in the case of FEM, the generation of the mesh still demands a considerable computational cost, especially when dealing with three-dimensional problems, in which surface elements need to be used.

It is noticeable that part of the limitations presented by the classic methods occur due to the need of a connectivity between the nodes. To overcome these limitations, a new class of methods, known as Mesh-free or Meshless, started to be developed. Overall, Mesh-free methods propose discretizing a structure using arbitrarily scattered nodes on the boundary and/or the domain of the body without using a mesh, that is, there is no need of connectivity between the nodes in order for the variables to be approximated, see Liu and Gu [3]. Thus, updating the topology of the discretization is reduced to removing, adding or changing the coordinates of nodes, diminishing the need of human intervention in the discretization process, as pointed out by Oliveira Jr. [4] and Oliveira et al. [5].

The present work proposes a new Boundary Mesh-Free Model (BMFM), that combines the Boundary Integral Equations with the shape functions of the Moving Least Squares (MLS). Thus, BMFM both minimizes the use of discretization, limited to the boundary of the body, and eliminates the use of a mesh. At the end of the work, BMFM was applied to a benchmark problem in order to for its effectiveness to be assessed.

2 Moving Least Squares

The Moving Least Squares (MLS) approximation is based on three elements: a complete set of polynomial base functions, a set of coefficients that are function of the space coordinates and a weight function of compact support associated with each node, see Atluri and Zhu [6].

Let Γ be the boundary of a two-dimensional domain Ω and consider a set of $N = \{x_1, x_2, ..., x_n\}$ nodal points of a mesh-free discretization. Local compact supports centered at each node are considered. In a neighborhood of a sampling point $\boldsymbol{x}$, the domain of definition Ω_x, over which the MLS approximation is defined, covers all the nodes whose compact supports include $\boldsymbol{x}$. Thus, the domain of definition is a direct consequence of the compact support of each node, where the respective MLS shape function is defined.

2.1 Shape functions

Consider the domain of definition Ω_x of a point $\boldsymbol{x}$. The MLS approximation of a scalar variable, over a number of scattered nodes $\boldsymbol{x_i}$, where the nodal parameter $\hat{u}_i$ is defined, is given by

$$u^h(\boldsymbol{x}) = \sum_{i=1}^{n} p_i(\boldsymbol{x}) a_i(\boldsymbol{x}) = \boldsymbol{p^T}(\boldsymbol{x})\boldsymbol{a}(\boldsymbol{x}), \tag{1}$$

in which $\boldsymbol{a}(\boldsymbol{x})$ is the vector of unknown coefficients that are functions of the space coordinates and $\boldsymbol{p^T}(\boldsymbol{x})$ is a vector of the complete monomial basis of order m. The vector $\boldsymbol{a(x)}$ is determined by minimizing the J(x) norm

$$J(\boldsymbol{x}) = \frac{1}{2}\sum_{i=1}^{n} w_i(\boldsymbol{x})[u^h(\boldsymbol{x}) - \hat{u}_i]^2 = \frac{1}{2}\sum_{i=1}^{n} w_i(\boldsymbol{x})[\boldsymbol{p^T}(\boldsymbol{x_i})\boldsymbol{a}(\boldsymbol{x}) - \hat{u}_i]^2 \tag{2}$$

with respect to each term of $\boldsymbol{a}(\boldsymbol{x})$. $w_i(\boldsymbol{x})$ is the weight function associated with the node $\boldsymbol{x_i}$, with compact support, that is $|w_i(\boldsymbol{x}) > 0|$ for all $\boldsymbol{x}$ in the support of $w_i(\boldsymbol{x})$. The minimization process leads to

$$\boldsymbol{A}(\boldsymbol{x})\boldsymbol{a}(\boldsymbol{x}) = \boldsymbol{B}(\boldsymbol{x})\hat{\boldsymbol{u}}, \tag{3}$$

in which

$$\boldsymbol{A}(\boldsymbol{x}) = \sum_{i=1}^{n} w_i(\boldsymbol{x})\boldsymbol{p}(\boldsymbol{x})\boldsymbol{p^T}(\boldsymbol{x}), \tag{4}$$

$$\boldsymbol{B}(\boldsymbol{x}) = [w_1(\boldsymbol{x})\boldsymbol{p}(\boldsymbol{x}_1), w_2(\boldsymbol{x})\boldsymbol{p}(\boldsymbol{x}_2), ..., w_n(\boldsymbol{x})\boldsymbol{p}(\boldsymbol{x}_n)], \tag{5}$$

$$\hat{\boldsymbol{u}} = [\hat{u}_1, \hat{u}_2, ..., \hat{u}_n]. \tag{6}$$

Solving eq. (3) for $\boldsymbol{a}(\boldsymbol{x})$ yields

$$\boldsymbol{a}(\boldsymbol{x}) = \boldsymbol{A}^{-1}(\boldsymbol{x})\boldsymbol{B}(\boldsymbol{x})\hat{\boldsymbol{u}}, \tag{7}$$

provided n $\geq$ m for each sampling point $\boldsymbol{x}$ as a necessary condition for a well-defined approximation. Substituting $\boldsymbol{a}(\boldsymbol{x})$ into eq. (1) leads to the final MLS approximation

$$u^h(\boldsymbol{x}) = \sum_{i=1}^{n} \phi_i(\boldsymbol{x})\hat{u}_i, \tag{8}$$

in which

$$\phi_i(\boldsymbol{x}) = \sum_{j=1}^{m} p_j(\boldsymbol{x})[\boldsymbol{A}^{-1}(\boldsymbol{x})\boldsymbol{B}(\boldsymbol{x})]_{ji} \tag{9}$$

is the shape function corresponding to the node $\boldsymbol{x_i}$.It is important to notice that the MLS approximations are not nodal interpolants, which means that $\phi_i(\boldsymbol{x}) \neq \delta_{ij}$.

2.2 Weight functions

Weight functions $w_i(\boldsymbol{x})$, introduced in eq. (4) and eq. (5), have a compact support which defines the subdomain where $|w_i(\boldsymbol{x}) > 0|$. This paper considers a quartic spline weight function, defined as

$$w_i(\boldsymbol{x}) = \begin{cases} 1 - 6\left(\frac{d_i}{r_i}\right)^2 + 8\left(\frac{d_i}{r_i}\right)^3 - 3\left(\frac{d_i}{r_i}\right)^4 & 0 \leq d_i \leq r_i \\ 0 & \text{otherwise} \end{cases}, \tag{10}$$

in which $d_i = \|\boldsymbol{x} - \boldsymbol{x}_i\|$. The parameter r_i is the size of the compact support of the weight function, defined as a dimensionless parameter α_s multiplied by the greatest distance between neighbouring nodes.

3 Boundary Integral Equations

Consider a 2D domain Ω with boundary $\Gamma = \Gamma_u \cup \Gamma_q$ where the potential is defined by the Laplace equation

$$\nabla^2 u = 0 \ \text{ on the domain } \Omega, \tag{11}$$

with the following boundary conditions

$$u(\boldsymbol{x}) = \bar{u} \ \text{ on } \Gamma_u, \tag{12}$$

$$q(\boldsymbol{x}) = \bar{q} \ \text{ on } \Gamma_q, \tag{13}$$

in which u($\boldsymbol{x}$) and q($\boldsymbol{x}$) are, respectively, the potential and the flux functions, while $\bar{u}$ and while $\bar{q}$ are the corresponding prescribed values; $\boldsymbol{n}$ is the outward unit normal to the boundary at point $\boldsymbol{x}$.

Applying the weighted residuals technique to eq. (11), considering an arbitrary weight u^* and integrating the result by parts twice leads to the transposed form of the Laplace equation

$$\int_\Omega (\nabla^2 u^*) u d\Omega + \int_\Gamma q^* u d\Gamma = \int_\Gamma u^* q d\Gamma, \tag{14}$$

in which $q^* = du/d\boldsymbol{n}$.

3.1 Fundamental solution and Boundary Integral Equations

The fundamental solution of the Laplace equation is defined on an infinite domain and represents the action of a concentrated unit charge, represented by the Dirac delta function Δ^i, applied at an arbitrary source point i, and is represented as

$$\nabla^2 u + \Delta^i = 0. \tag{15}$$

The solution of eq. (15) leads to the fundamental solutions of the potential and the flux, respectively given by

$$u^* = \frac{1}{2\pi} ln\left(\frac{1}{r}\right), \tag{16}$$

$$q^* = \frac{\partial u^*}{\partial \boldsymbol{n}} = -\frac{1}{2\pi r}\frac{\partial r}{\partial \boldsymbol{n}}, \tag{17}$$

in which r represents the distance between the source point $\boldsymbol{x_i}$ and the field point $\boldsymbol{x}$.

Substituting eq. (15) in eq. (14) leads to

$$u^i + \int_\Gamma q^* u d\Gamma = \int_\Gamma u^* q d\Gamma. \tag{18}$$

When the source point is on the boundary, eq. (18) leads to

$$c^i u^i + \int_\Gamma q^* u d\Gamma = \int_\Gamma u^* q d\Gamma. \tag{19}$$

in which c^i is a constant that can be calculated implicitly, see Brebbia and Dominguez [7].

4 Boundary Mesh-Free Model

The proposed Boundary Mesh-Free Model (BMFM) is introduced in this chapter. It is important to notice that the method is based on the Boundary Node Method, see Mukherjee and Mukherjee [8], that also combines the Boundary Integral Equations with the MLS shape functions. However, the methods differ in the way the boundary is discretized, the way the MLS is applied to generate the shape functions, the form that the final system of equations is assembled, and the MLS weight function utilized.

Consider a two-dimensional domain Ω with boundary $\Gamma = \Gamma_u \cup \Gamma_q$ where the potential problem is defined by the Laplace equation, eq. (11), and with boundary conditions as defined in eq. (12) and eq. (13). BMFM performs the discretization of the boundary with N segments Γ_j. Each segment has an arbitrary set of internal nodes n_j linked by linear sub-segments. Boundary corners are free of nodes, as illustrated in Fig. 1. The MLS is applied independently on each segment Γ_j to approximate the potential u and the flux q, as

$$u = \boldsymbol{\Phi}_j \hat{\boldsymbol{u}}^j, \tag{20}$$

$$q = \boldsymbol{\Phi}_j \hat{\boldsymbol{q}}^j, \tag{21}$$

in which $\hat{\boldsymbol{u}}^j$ and $\hat{\boldsymbol{q}}^j$ are the potential and the flux parameters of the n_j nodes of the segment Γ_j ; and $\boldsymbol{\Phi}_j$ is the vector of shape functions of nodes included in the definition domain of point $\boldsymbol{x}$, expanded with zero entries for remaining nodes of the segment. Hence, the MLS approximation of eq. (19) leads to

$$c^i \boldsymbol{\Phi}_j^i \hat{\boldsymbol{u}}^j + \sum_{j=1}^{N} \int_{\Gamma_j} q^* \boldsymbol{\Phi}_j d\Gamma \hat{\boldsymbol{u}}^j = \sum_{j=1}^{N} \int_{\Gamma_j} u^* \boldsymbol{\Phi}_j d\Gamma \hat{\boldsymbol{q}}^j \quad \text{or} \tag{22}$$

$$(\boldsymbol{C}^i + \boldsymbol{H}^i)\hat{\boldsymbol{U}} = \boldsymbol{G}^i \hat{\boldsymbol{Q}}, \tag{23}$$

in which $\hat{\boldsymbol{U}}$ and $\hat{\boldsymbol{Q}}$ represent the nodal parameters of potential and flux of the n_j nodes of the segment Γ_j, and $\boldsymbol{H}^i$, $\boldsymbol{C}^i$ and $\boldsymbol{G}^i$ are, respectively

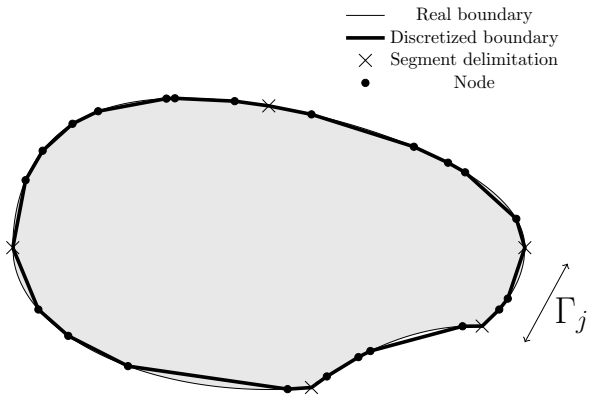

Figure 1. BMFM discretization of the boundary Γ, defined with N segments Γ_j

$$\boldsymbol{H}^i = \sum_{j=1}^{N} \int_{\Gamma_j} q^* \boldsymbol{\Phi}_j d\Gamma, \tag{24}$$

$$\boldsymbol{C}^i = c^i \boldsymbol{\Phi}_j^i, \tag{25}$$

$$\boldsymbol{G}^i = \sum_{j=1}^{N} \int_{\Gamma_j} u^* \boldsymbol{\Phi}_j d\Gamma. \tag{26}$$

Once eq. (23) is applied to all i boundary nodes and the numerical integration (using Gaussian quadrature for nodes that are far from the singularity and the logarithmic Gaussian quadrature for those near the singularity) is finished, the global system can be written as

$$(\boldsymbol{C} + \boldsymbol{H})\hat{\boldsymbol{U}} = \boldsymbol{G}\hat{\boldsymbol{Q}}, \tag{27}$$

in which $\hat{\boldsymbol{U}}$ and $\hat{\boldsymbol{Q}}$ represent the nodal parameters of potential and flux of all the boundary nodes, and $\boldsymbol{H}$, $\boldsymbol{C}$ and $\boldsymbol{G}$ are the global coefficient matrixes. Since $\hat{\boldsymbol{U}}$ and $\hat{\boldsymbol{Q}}$ do not represent the nodal approximation values, the imposition of boundary constraints is done by rearranging eq. (27), leading to

$$\begin{bmatrix} (\boldsymbol{C} + \boldsymbol{H}) & -\boldsymbol{G} \\ \boldsymbol{\Phi}_{\hat{U}} & \boldsymbol{0} \\ \boldsymbol{0} & \boldsymbol{\Phi}_{\hat{Q}} \end{bmatrix} \begin{bmatrix} \hat{\boldsymbol{U}} \\ \hat{\boldsymbol{Q}} \end{bmatrix} = \begin{bmatrix} \boldsymbol{0} \\ \boldsymbol{U} \\ \boldsymbol{Q} \end{bmatrix} \tag{28}$$

in which $\boldsymbol{\Phi}_{\hat{U}}$ and $\boldsymbol{\Phi}_{\hat{Q}}$ are the matrixes of the MLS shape functions of the nodes with prescribed values potential $\boldsymbol{U}$ and fluxes $\boldsymbol{Q}$, respectively.

Finally, the system of equations presented in eq. (28) can be solved for $\boldsymbol{\Phi}_{\hat{U}}$ and $\boldsymbol{\Phi}_{\hat{Q}}$. Once the nodal parameters are known, it is possible to approximate u and q in any boundary point using eq. (8) and eq. (18) can be applied to obtain the potential and fluxes on internal points.

5 Numerical results

BMFM was applied to a benchmark problem. The average relative error (E_m) was estimated using eq. (29). The points in which $u^i_{analytical} = 0$ were not considered in the calculation of the error.

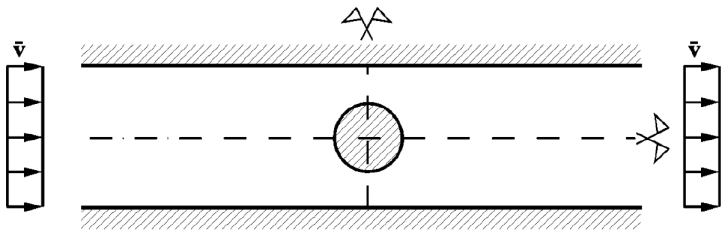

Figure 2. Benchmark problem – potential flow over a circular cylinder

$$E_m = \frac{1}{n}\sum_{j=1}^{N}\left|\frac{u^i_{analytical} - u^i_{BMFM}}{u^i_{analytical}}\right| \tag{29}$$

The benchmark problem considers the potential flow of an ideal fluid in a rectangular channel over a circular cylinder, as illustrated in Fig. 2. Due to symmetry, only a quarter of the problem needs to be analyzed. The considered geometry and boundary conditions are illustrated in Fig. 3a. The analytical solution of the problem is given in eq. (30). The BMFM discretization consisted of 34 nodes, distributed according to Fig. 3b. The ends of all segments, represented by an x, are free of nodes. A cubic polynomial base was used (m=4) and α_s = 12.4. The numerical results are presented in Fig. 4 for the potential and Fig. 5 for the fluxes. It is very clear by the graphs and their E_m errors that the BMFM obtained results extremely close to the analytical ones.

$$u(x,y) = x\left(1 + \frac{1}{x^2+y^2}\right). \tag{30}$$

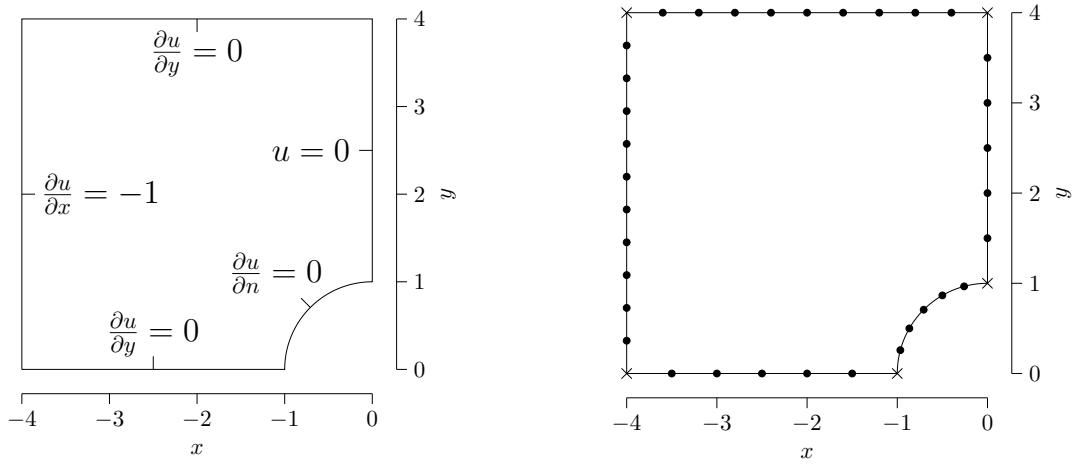

(a) (b)

Figure 3. (a) Domain and boundary conditions considered (b) BMFM discretization of the problem

6 Conclusions

The present work aims to introduce a new formulation of a Boundary Mesh-Free Model, based on the Boundary Node Method, using the Boundary Integral Equations and the MLS shape functions. Therefore, BMFM eliminates the need of a mesh, reducing the discretization process to randomly positioning nodes on the boundary of the body. To assess the effectiviness of the method, it was applied to a benchmark problem. BMFM lead to results

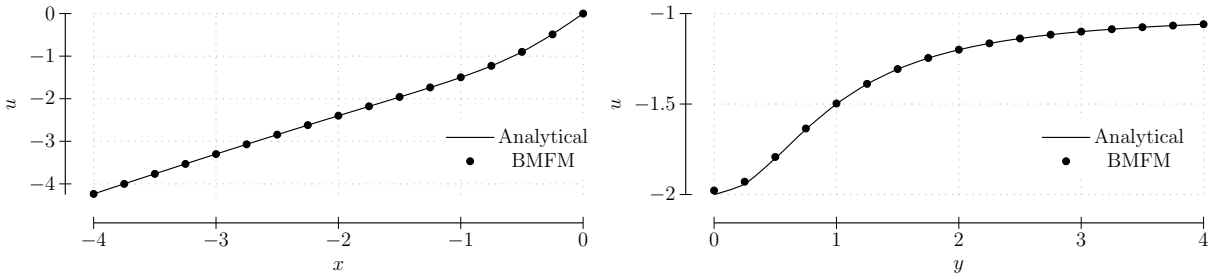

(a) (b)

Figure 4. Potential at section at (a) y= 1, E_m =0.11% (b) x= -1, E_m =0.18%

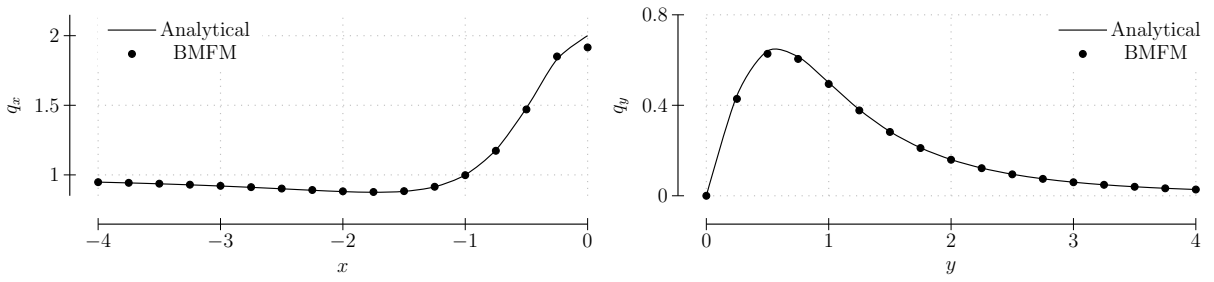

(a) (b)

Figure 5. (a) Horizontal flux at section y=1, E_m =0.50% (b) Vertical flux at section at x=-1, E_m =0.83%

with very small errors when compared to the analytical results, which shows how robust and reliable the method is. It is important to notice that the method is not only promising due to its great results, but also because of how simple its discretization process is, which allows for minimal human intervention on the process. Thus, it is clear that BMFM can be a good alternative to more classic, mesh-based numerical methods.

Acknowledgements. The authors of this paper acknowledge the financial support given by CAPES.

Authorship statement. The authors hereby confirm that they are the sole liable persons responsible for the authorship of this work, and that all material that has been herein included as part of the present paper is either the property (and authorship) of the authors, or has the permission of the owners to be included here.

References

[1] Andújar, R., Jaume, R., & Vojko, K., 2011. Beyond fem: overview on physics simulation tools for structural engineers. *Technics Technologies Education Management*, vol. 6.3, pp. 555–571.
[2] Gaul, L., Kogl, M., & Wagner, M., 2003. *Boundary Element Methods for engineers and scientists, 1st Ed.* Springer-Verlag Berlin Heidelberg.
[3] Liu, G. R. & Gu, Y. T., 2003. A meshfree method: Meshfree weak–strong (mws) form method, for 2-d solids. *Computational Mechanics*, vol. 33, pp. 2–14.
[4] Oliveira Jr., V. G., 2015. *Formulação cinemática local de métodos sem malha*. Masters dissertation, Departamento de Engenharia Civil e Ambiental, Universidade de Brasília.
[5] Oliveira, T., Vélez, W., Santana, E., Araújo, T., Mendonça, A., & PORTELA, A., 2019. A local mesh free method for linear elasticity and fracture mechanics. *Engineering Analysis with Boundary Elements*, vol. 101, pp. 221–242.
[6] Atluri, S. & Zhu, T., 2000. New concepts in meshless methods. *International Journal for Numerical Methods in Engineering*, vol. 47, pp. 537–556.
[7] Brebbia, C. & Dominguez, J., 1992. *Boundary Elements An Introductory Course, 2nd Ed.* WIT Press, Ashurst Lodge, UK.
[8] Mukherjee, Y. & Mukherjee, S., 1998. The boundary node method for potential problems. *International Journal for Numerical Methods in Engineering*, vol. 40.5.